Artificial Chaperones

DOI: 10.1002/ange.201400735

Maintenance of Amyloid β Peptide Homeostasis by Artificial Chaperones Based on Mixed-Shell Polymeric Micelles**

*Fan Huang, Jianzu Wang, Aoting Qu, Liangliang Shen, Jinjian Liu, Jianfeng Liu, Zhenkun Zhang, Yingli An, and Linqi Shi**

Abstract: *The disruption of Aβ homeostasis, which results in the accumulation of neurotoxic amyloids, is the fundamental cause of Alzheimer's disease (AD). Molecular chaperones play a critical role in controlling undesired protein misfolding and maintaining intricate proteostasis in vivo. Inspired by a natural molecular chaperone, an artificial chaperone consisting of mixed-shell polymeric micelles (MSPMs) has been devised with tunable surface properties, serving as a suppressor of AD. Taking advantage of biocompatibility, selectivity toward aberrant proteins, and long blood circulation, these MSPM-based chaperones can maintain Aβ homeostasis by a combination of inhibiting Aβ fibrillation and facilitating Aβ aggregate clearance and simultaneously reducing Aβ-mediated neurotoxicity. The balance of hydrophilic/hydrophobic moieties on the surface of MSPMs is important for their enhanced therapeutic effect.*

Alzheimer's disease (AD) is an irreversible, devastating, and progressive neurodegenerative disorder that affects millions of people around the world.[1] Although available drugs can temporarily alleviate the condition of the patient, currently there are no effective treatments that can suppress or cure the disease. The cerebral extracellular amyloid plaques and intracellular neurofibrillary tangles, comprising of amyloid β peptides (Aβ) and tau proteins, respectively, are considered as two pathological hallmarks of AD.[2] It is generally accepted that the aggregation of monomeric Aβ into insoluble plaque-associated amyloid fibrils is a crucial step that drives AD pathogenesis.[3] Based on this hypothesis regarding amyloids, extensive efforts have been dedicated to developing Aβ inhibitors, such as small molecules[4] and peptides,[5] metal-ion chelators,[6] antibodies,[7] and various nanoparticles (NPs),[8] which display certain beneficial effects on AD treatment by blocking Aβ aggregation. However, the therapeutic effect could not be completely achieved if only considered from the perspective of suppressing Aβ accumulation. In fact, the imbalance between Aβ anabolism and catabolism in the central nervous system (CNS) is the primary event responsible for the pathology of AD.[9] In healthy brains, the production of Aβ is normally in equilibrium with its clearance. Both overproduction and underclearance could disrupt Aβ homeostasis, thus resulting in increasing amounts of Aβ, which could further induce diverse amyloid aggregates with different toxicities and ultimately lead to neuronal damage and cell death. Moreover, a growing body of recent evidence suggests that soluble oligomers preceding fibril formation are the most toxic species of all forms of Aβ aggregates.[10] Thus, an attractive therapeutic strategy for AD treatment would be the effective maintenance of Aβ homeostasis by a combination of inhibiting Aβ aggregation and promoting Aβ aggregate clearance, and simultaneously diminishing Aβ oligomer neurotoxicity. This strategy has not yet been realized, especially on a single nanoplatform.

Molecular chaperones, as an important part of the cellular quality control system, play a pivotal role in controlling undesired protein misfolding and maintaining intricate proteostasis in vivo.[11] A number of chaperones have been described with the ability to provide a firm line of defense against neurodegenerative diseases, including human chaperone Hsp70, apolipoprotein E (apoE), and clusterin.[12] Typically, the chaperone machinery binds to exposed hydrophobic residues of non-native proteins to form stable complexes and, by doing so, prevent the unfavorable aggregation that harms the proteostasis and "detoxify" the protein aggregates. Furthermore, chaperones are also involved in the disassembly of protein aggregates and facilitate the proteolytic digestion of abnormal proteins. Therefore, molecular chaperones are competent to fulfill all above-mentioned attributes for the treatment of AD, and it is very compelling and promising to develop efficient artificial chaperones to reduce the Aβ burden in the brain.

Herein, we fabricate a simple and biocompatible MSPM with tunable surface properties as an artificial chaperone that can potently maintain Aβ homeostasis and reduce Aβ-mediated toxicity. This MSPM-based chaperone is obtained by the straightforward self-assembly of two amphiphilic diblock copolymers, poly(ε-caprolactone)-*block*-poly(ethylene oxide) (PCL-*b*-PEG) and poly(ε-caprolactone)-*block*-poly(N-isopropylacrylamide) (PCL-*b*-PNIPAM) in aqueous

[*] F. Huang, J. Wang, A. Qu, L. Shen, Dr. Z. Zhang, Y. An, Prof. L. Shi
Key Laboratory of Functional Polymer Materials, Ministry of Education, Collaborative Innovation Center of Chemical Science and Engineering (Tianjin), Institute of Polymer Chemistry, State Key Laboratory of Medicinal Chemical Biology, Nankai University
Tianjin, 300071, (P.R. China)
Institution
E-mail: shilinqi@nankai.edu.cn
Dr. J. Liu, J. Liu
Tianjin Key Laboratory of Radiation Medicine and Molecular Nuclear Medicine, Institute of Radiation Medicine, Chinese Academy of Medical Science & Peking Union Medical College
Tianjin, 300192, (P.R. China)

[**] This work was financially supported by the National Natural Science Foundation of China (Nos. 91127045, 51390483, 21274067, 81171371, 51203189), the National Basic Research Program of China (973 Program, No. 2011CB932503), and PCSIRT (IRT1257).

Supporting information for this article is available on the WWW under http://dx.doi.org/10.1002/anie.201400735.

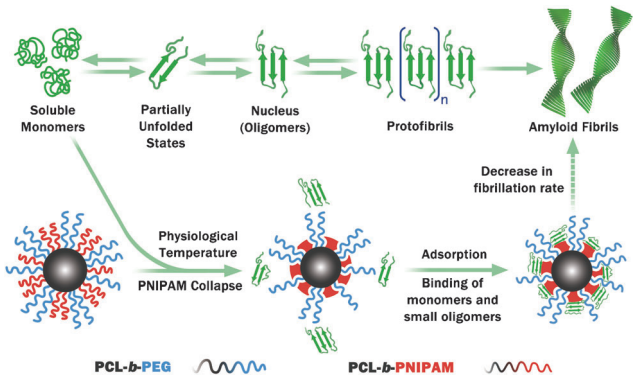

Scheme 1. Representation of the possible mechanism of interaction between MSPMs and Aβ peptide on the kinetics of amyloid fibrillation process.

solution (Scheme 1), resulting in complex micelles with a PCL core and a mixed shell that consists of PEG and PNIPAM. By raising the temperature up to the normal physiological temperature of the human body, the PNIPAM chains in the micellar shell will spontaneously undergo a hydrophilic to hydrophobic transformation and collapse, thus forming hydrophobic domains on the PCL core. These hydrophobic domains may act as anchors for interacting with hydrophobic Aβ monomers or its intermediate oligomeric aggregates, while the hydrophilic and stretched PEG chains could create a protective barrier layer to prevent excessive amounts of Aβ adsorption and the aggregation of micelles themselves. More importantly, the area of the PNIPAM domain can be precisely tuned by variation of the ratio of the two copolymers. In this way, it is very convenient to modulate the surface properties of the MSPMs and control the effect of MSPMs on the Aβ fibrillation progress. In our previous work, we have demonstrated that, under physiological conditions, such MSPMs will not interact with and interrupt the function of a wide range of normal proteins.[13,14] They only selectively target aberrant proteins with exposed hydrophobic moieties, among which Aβ is a typical example. Furthermore, MSPMs with the proper balance of hydrophilicity and hydrophobicity on the surface have the advantageous property of long blood circulation,[14] which is critical for the future practical application of any Aβ inhibitor.

The soluble monomeric form of an Aβ peptide undergoes specific conformational transitions into aggregation-prone "partially unfolded intermediates" and subsequently aggregates into toxic oligomers (nucleus) through the β-domain (Scheme 1). These transient oligomers have been regarded as the most toxic species, as they serve as a template for further Aβ deposition, resulting in rapid fibril growth and eventually in the formation of insoluble mature amyloid fibrils, driven by intermolecular associations. While in the presence of the functional state of MSPMs, the partially unfolded state of the monomers and other small intermediate units can bind to the surface of the micelle, benefiting from the synergic effect of hydrophilic PEG chains and hydrophobic PNIPAM domains, thus leading to the formation of MSPM-peptides complexes that are stabilized by the stretched PEG chains. This progress could block active sites hidden in the Aβ hydrophobic core that is responsible for the aggregation. Furthermore, owing to the high affinity for the micellar surface, binding will lead to a decrease of Aβ monomer concentration in the solution, which disturbs the dynamic equilibrium between monomeric and oligomeric species. Consequently, MSPM-based chaperones are expected to significantly inhibit the transition from the native state into β-sheet secondary structure and frustrate Aβ fibrillation.

To investigate the effect of MSPMs on Aβ fibrillation, the thioflavin-T (ThT) fluorescence assay was adopted to monitor the formation of amyloid fibrils. As seen in Figure 1 a, when fresh Aβ was incubated alone at 37 °C, the time-dependent change of the ThT fluorescence intensity (FI) exhibited

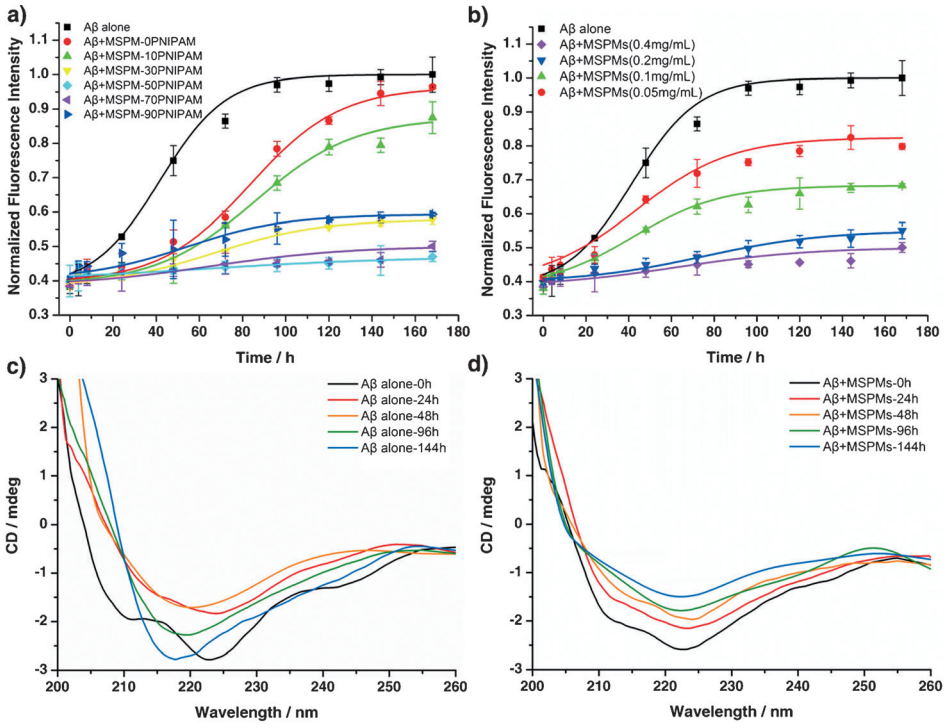

Figure 1. Inhibition of Aβ fibrillation by MSPMs. a) Fibrillation kinetics of Aβ in the absence and presence of MSPMs (0.4 mg mL^{-1}) with different PCL-*b*-PEG/PCL-*b*-PNIPAM ratios. b) Fibrillation kinetics of Aβ in the presence of MSPM-70PNIPAM with various concentrations. The fibrillation kinetics of Aβ was measured by ThT binding assay. Data are presented as mean ± SD, $n = 3$. c) CD spectra of Aβ alone incubated at 37 °C at different time points of the fibrillation process. d) CD spectra of Aβ in the presence of MSPM-70PNIPAM incubated at 37 °C at different time points of the fibrillation process.

a sigmoidal kinetic form, as widely observed before.[8a] This result indicates that the progress of Aβ fibrillation follows a typical nucleation-growth mode that consists of three stages: lag phase, elongation phase, and stationary phase.[15] The saturation of the ThT FI after approximately 90 h indicates that all of the Aβ end up in the form of fibrils (also see Figure 2c). Upon the introduction of MSPMs, the

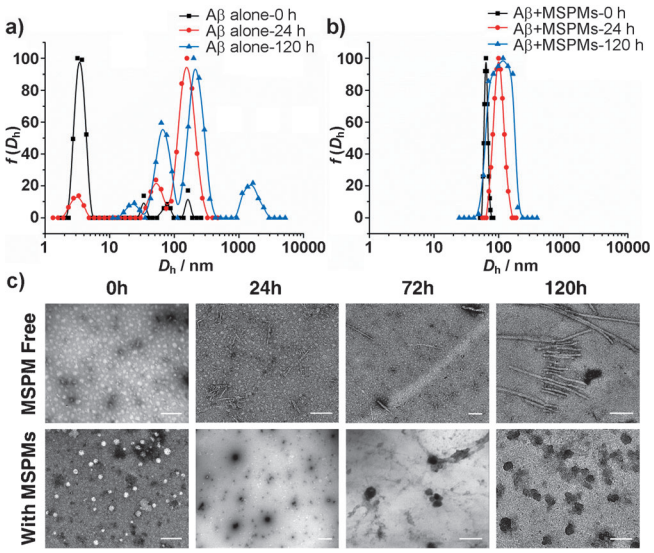

Figure 2. Temporal evolution of the size distribution of Aβ in the absence (a) and presence (b) of MSPMs incubated at 37 °C, as probed by dynamic light scattering. c) TEM images of Aβ incubated with and without MSPMs at different time points of the fibrillation process. The PCL-*b*-PEG/PCL-*b*-PNIPAM ratio in the MSPMs was 3:7 (*w*/*w*). [Aβ] = 20 μM, [MSPMs] = 0.4 mg mL^{-1}. Buffer: 10 mM PBS, pH 7.4 (scale bar: 200 nm).

lag phase extended and the FI at saturation decreased, indicating that the MSPM-based chaperone can effectively suppress the Aβ fibrillation process. Moreover, there is an intriguing observation that different proportion of hydrophilic and hydrophobic segments in the micellar shell has different inhibitory effect. The simple micelles consisting of only PCL-*b*-PEG (MSPM-0PNIPAM) temporarily increased the lag time of fibrillation while the ThT FI eventually approached that of the pure Aβ. This finding suggests that there exists certain interaction between Aβ and MSPM-0PNIPAM despite the fact that they cannot prevent Aβ fibril formation. In the cases of other MSPMs, the lag time significantly increased and the elongation rate remarkably declined with an increasing amount of PNIPAM, implying that the inhibitory effect was enhanced. This phenomenon strongly highlights the importance of PNIPAM in the retardation of Aβ aggregation. However, it is worth noting that MSPM-90PNIPAM has lower efficiency than MSPM-30, 50, 70PNIPAM. Among all of the MSPMs with various PEG/PNIPAM ratios (w/w), MSPM-50PNIPAM exhibited the best inhibition ability. Thus, excessive PNIPAM does not mean a more notable inhibitory effect and it seems that the delicate balance between PEG chains and PNIPAM domains play a crucial role in preventing Aβ self-aggregation. Furthermore, MSPMs hindered the Aβ aggregate formation in a concentration-dependent manner (Figure 1b): the higher concentration of MSPMs, the greater inhibitory ability for Aβ fibrillation. Furthermore, our data (Supporting Information, Figure S1) showed that these MSPMs could reverse Aβ aggregation at early stages of the fibrillation progress but had no effect if mature fibrils formed. This result is consistent with the work of Dawson and co-workers.[8a]

Far-UV circular dichroism (CD) spectroscopy was performed to monitor the secondary structure change during the Aβ fibrillation progress, both in the absence and presence of MSPMs (Figure 1c,d). At first, both fresh Aβ alone and MSPMs/Aβ mixture adopted a predominant α-helical structure with two negative bands around 208 and 222 nm, which are characteristics of α-helical conformation.[16] After 24 h intubation at 37 °C, the CD spectrum for Aβ alone showed a sharp decrease of intensity at 222 nm and the 208 nm peak disappeared, which was indicative of transition state from α-helical into β-sheet. When the incubation was prolonged to 48 h, its spectral shape shifted the minimum from 222 to 217 nm, signifying a typical β-sheet-rich structure.[17] Moreover, its relative intensity at 217 nm, which represented the content of β-sheet, became increasingly pronounced as the incubation time further increased. In contrast, Aβ in the presence of MSPMs exhibited α-helical structure for 48 h and finally fixed in the transition states during the incubation time. The CD results strongly suggested that the MSPMs could hinder the conformation transition of Aβ from α-helical to β-sheet, confirming the interactions between Aβ and MSPMs.

To further verify the achieved inhibitory effect of MSPMs on Aβ aggregation and corroborate the aforementioned mechanism, dynamic light scattering (DLS) and transmission electron microscopy (TEM) were exploited to detect the time evolution of the size distribution and morphology changes in Aβ solution, respectively.[18,19] Figure 2a clearly shows the overall Aβ polymerization progress (Supporting Information, Figure S2). Immediately on Aβ dissolution, the size distributions predominantly comprised of particles with an average hydrodynamic diameter (D_h) of around 10 nm, which was consistent with the size of Aβ monomeric state. Over time, the scattering intensity of the small particles sharply decreased and larger aggregates emerged. Moreover, the average D_h for the larger aggregates increased with time (Supporting Information, Table S2), corresponding to significant Aβ fibril formation. Whereas in the case of the MSPMs/Aβ mixture, the D_h value was similar to that of MSPMs alone at first, then increased from 65 nm to 98 nm with narrow size distribution, indicating the formation of homogeneous MSPM-Aβ complexes. Notably, the D_h of MSPM-Aβ complexes had little variation in this time period. Meanwhile, Aβ fibrillation progress can be observed by TEM (Figure 2c). As time elapsed, Aβ self-organized into larger aggregates gradually, including oligomers and protofibrils, and finally formed mature fibrils with lengths of several micrometers. On the other hand, in a mixture of Aβ and MSPMs, no any fibrous aggregates could be found during the incubation time. Furthermore, it should be note that the MSPM-Aβ complexes presented black spherical structure which were distinct from

those white MSPMs (Supporting Information, Figure S4), providing the evidence of Aβ adsorption by MSPMs. All these observations demonstrated that our MSPMs could effectively block Aβ aggregation through trapping Aβ monomers and small oligomers onto their tunable surface.

On the basis of the above results, measurements with a quartz crystal microbalance with dissipation monitoring (QCM-D) were employed to further investigate the binding affinity of MSPMs for Aβ (Supporting Information, Figure S6).[20] After a stable baseline had been established, the surface-bound MSPMs with different hydrophilic/hydrophobic ratios were exposed to the Aβ solution at 37 °C, resulting in a rapid decrease in resonant frequency, which indicated that Aβ bind to all types of MSPMs, including the simple micelles MSPM-0PNIPAM. Nevertheless, the amount of frequency attenuation (Δf) is smaller for MSPM-0PNIPAM than for the others. This result suggested that MSPM-0PNIPAM were capable of interacting with Aβ but their adhesion to the peptides was much weaker than other MSPMs. The largest decrease of Δf is MSPM-50PNIPAM, implying that MSPM-50PNIPAM had the strongest affinity for Aβ peptide in the series, in good agreement with ThT study that MSPM-50PNIPAM are the most efficiency in preventing Aβ fibrillation. Furthermore, all types of MSPMs prefer binding monomers to trapping oligomers and almost have no interaction with fibrils (Supporting Information, Figure S7 a–f). Recently, Nicolas et al.[21] reported that the outer PEG shell of NPs played a vital role for Aβ-NP interactions. It is therefore proposed that PEG chains triggered the uptake of Aβ by MSPMs and then the PNIPAM binding patches were able to strongly capture the peptides, highlighting the significance of synergic effect of hydrophilic PEG chains and hydrophobic PNIPAM domains in preventing Aβ assembly.

As our MSPMs can block Aβ aggregate formation by confining Aβ monomers or oligomers onto their surface, they should also be useful in inhibiting neurotoxicity exerted on the neuronal cells by the toxic Aβ species, a major reason for the neurodegenerative disorder. To test this, PC12 and SH-SY5Y cells were used as the neuronal model to evaluate the effect of MSPMs on cell viability and on Aβ-induced cytotoxicity. As shown in Figure 3 a, negligible cytotoxicity was observed for MSPMs with varying concentration from 6.25 to 400 μg mL^{-1}, suggesting the great biocompatibility of MSPMs. When incubation of PC cells with Aβ alone pre-incubated for 24 h at 37 °C already, the cell viability was reduced to about 40 % (Figure 3 c). In contrast, the survival of cells was increased to as high as about 80 % in the presence of

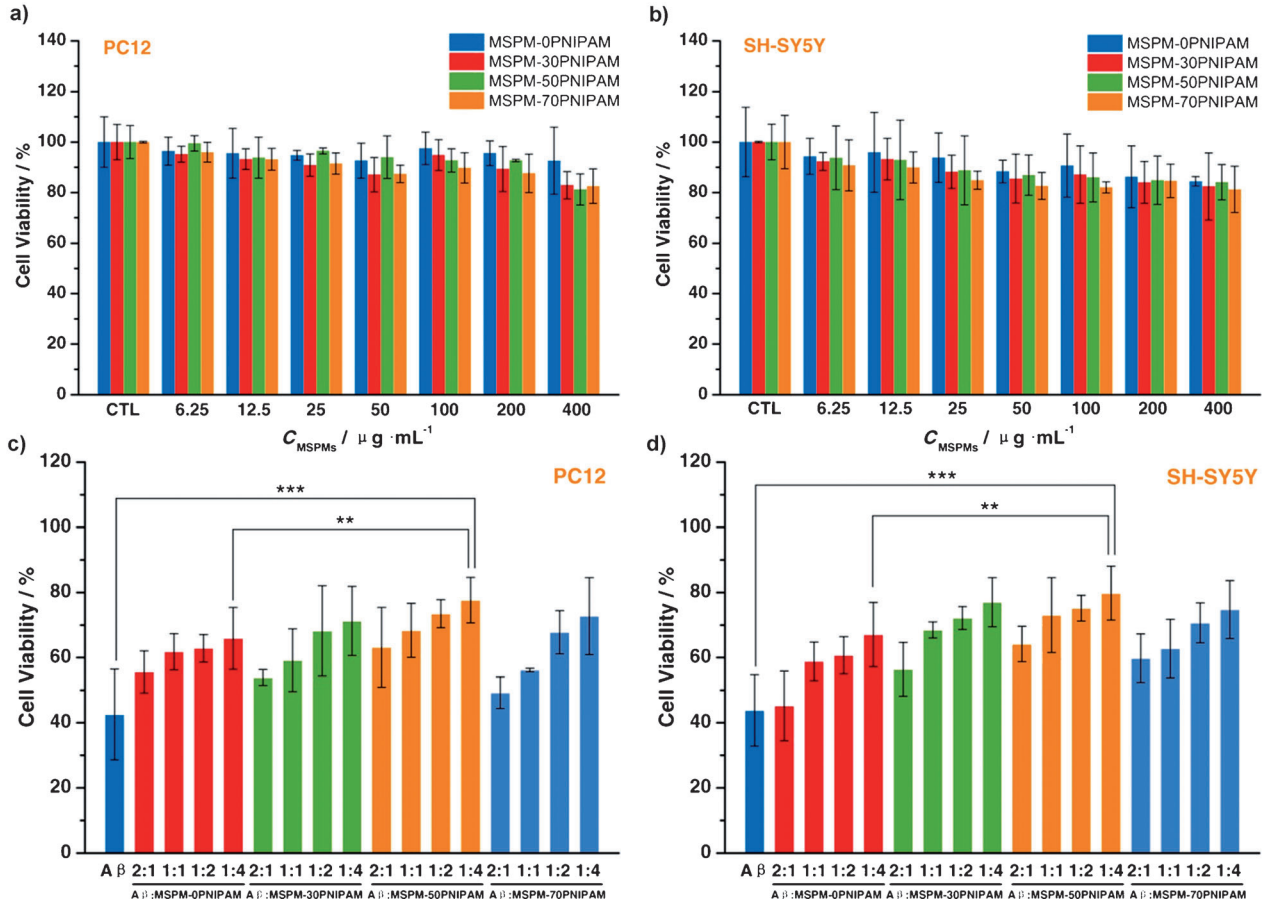

Figure 3. Reduction of Aβ neurotoxicity with MSPMs. a), b) Cytotoxicity of four different MSPMs (MSPM-0, 30, 50, 70PNIPAM) against two different cells: a) PC12 cells, b) SH-SY5Y cells. c), d) Effect of three different MSPMs with four different molar ratios (2:1, 1:1, 1:2, 1:4) on the cell toxicity of Aβ: c) PC12 cells, d) SH-SY5Y cells. Cell viability was measured by MTT assay and the data were shown as the mean ± SD of 6 replicate groups. Significance levels are expressed by asterisks: $^{**}P < 0.01$ and $^{***}P < 0.001$.

MSPMs, which demonstrated that MSPMs is able to protect cell viability from harmful Aβ aggregation. The simple micelles also affect cell survival but their protective effect is not as good as other MSPMs. This result may confirm that MSPMs are better than simple micelles in inhibiting cellular toxicity. Furthermore, it is important to point that, in agreement with ThT data, MSPMs reduced the neurotoxicity of Aβ is also consistent with concentration-dependent manner. Similar results have been obtained when SH-SY5Y cells were used (Figure 3b,d). Therefore, MSPMs not only showed excellent capacity to inhibit Aβ fibrillation by precisely tuning the surface properties, but also could substantially decrease Aβ-induced cytotoxicity.

Finally, owing to the fact that Aβ homeostasis is potently regulated by proteolytic degradation,[22] proteolysis experiments were applied to explore the degradation rate of mature amyloid fibrils and MSPM-Aβ complexes by proteinase K. The data obtained (Figure 4a) showed that ThT fluorescence intensity of MSPM-Aβ complexes was prominently decreased with time, whereas mature amyloid fibrils only cause a slight reduction in the first 16 h and then the relative fluorescence intensity started to increase. This demonstrates that MSPM-Aβ complexes were highly susceptible to degrade as compared to amyloid fibrils (Figure 4b), implying the favorable ability of MSPM-Aβ complexes to facilitate Aβ aggregate degradation.

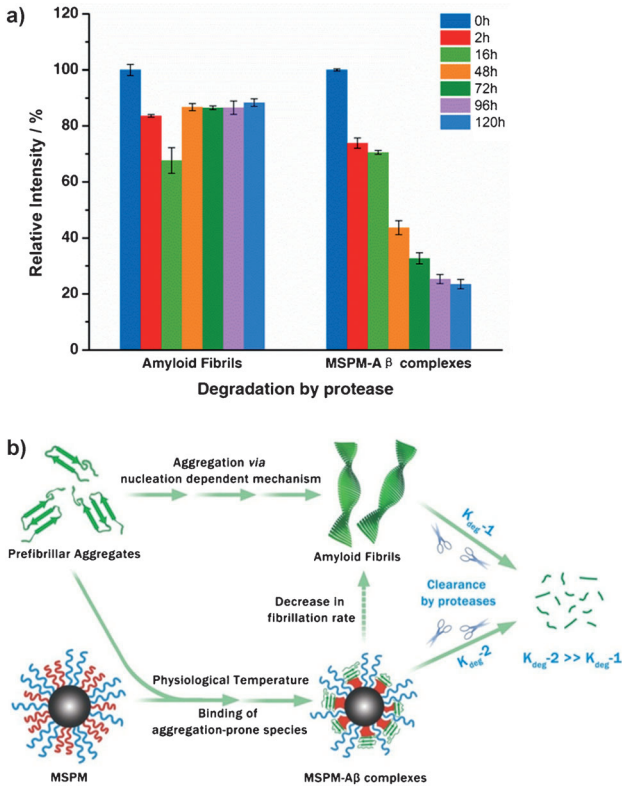

Figure 4. a) Degradation effect of amyloid fibrils and MSPMs-Aβ complexes by proteinase K using ThT fluorescence assay. The histogram has been normalized to the corresponding maximum value for each data. d) Illustration of the degradation of amyloid fibrils and MSPMs-Aβ complexes.

In summary, we have successfully designed and developed an innovative artificial molecular chaperone, MSPMs with tunable surface properties, which can serve as an excellent suppressor of AD. Through binding the aggregation-prone species of Aβ onto the tunable surface and forming spherical complexes, MSPMs can maintain the appropriate balance of Aβ levels by incorporating functions for both inhibiting Aβ fibrillation and facilitating Aβ aggregate degradation, and synchronously reduce the Aβ-related neurotoxicity. The synergic effect of hydrophilic chains and hydrophobic domains of MSPMs is the main factor in the MSPMs-Aβ interactions. Moreover, it is notable that proper balance between hydrophilic moieties and hydrophobic ones on the surface of MSPMs play a central role for showing enhanced therapeutic effect. Therefore, our results could provide new insights into the development of artificial chaperone as an ideal candidate for AD treatment.

Received: January 23, 2014
Revised: March 20, 2014
Published online: July 1, 2014

Keywords: amyloid β peptide · Alzheimer's disease · artificial chaperones · homeostasis · polymeric micelles

[1] a) M. P. Mattson, *Nature* **2004**, *430*, 631; b) K. Blennow, M. J. de Leon, H. Zetterberg, *The Lancet* **2006**, *368*, 387; c) T. Silva, J. Teixeira, F. Remião, F. Borges, *Angew. Chem.* **2013**, *125*, 1146; *Angew. Chem. Int. Ed.* **2013**, *52*, 1110.

[2] a) D. J. Selkoe, *Physiol. Rev.* **2001**, *81*, 741; b) M. Goedert, M. G. Spillantini, *Science* **2006**, *314*, 777; c) R. J. Perrin, A. M. Fagan, D. M. Holtzman, *Nature* **2009**, *461*, 916; d) R. Jakob-Roetne, H. Jacobsen, *Angew. Chem.* **2009**, *121*, 3074; *Angew. Chem. Int. Ed.* **2009**, *48*, 3030.

[3] a) F. Chiti, C. M. Dobson, *Annu. Rev. Biochem.* **2006**, *75*, 333; b) F. M. LaFerla, K. N. Green, S. Oddo, *Nat. Rev. Neurosci.* **2007**, *8*, 499; c) R. Roychaudhuri, M. Yang, M. M. Hoshi, D. B. Teplow, *J. Biol. Chem.* **2009**, *284*, 4749; d) I. W. Hamley, *Chem. Rev.* **2012**, *112*, 5147.

[4] a) F. Yang, G. P. Lim, A. N. Begum, O. J. Ubeda, M. R. Simmons, S. S. Ambegaokar, P. P. Chen, R. Kayed, C. G. Glabe, S. A. Frautschy, G. M. Cole, *J. Biol. Chem.* **2005**, *280*, 5892; b) A. Cavalli, M. L. Bolognesi, S. Capsoni, V. Andrisano, M. Bartolini, E. Margotti, A. Cattaneo, M. Recanatini, C. Melchiorre, *Angew. Chem.* **2007**, *119*, 3763; *Angew. Chem. Int. Ed.* **2007**, *46*, 3689.

[5] a) T. Takahashi, H. Mihara, *Acc. Chem. Res.* **2008**, *41*, 1309; b) D. J. Gordon, K. L. Sciarretta, S. C. Meredith, *Biochemistry* **2001**, *40*, 8237.

[6] a) P. J. Crouch, K. J. Barnham, *Acc. Chem. Res.* **2012**, *45*, 1604; b) S. S. Hindo, A. M. Mancino, J. J. Braymer, Y. Liu, S. Vivekanandan, A. Ramamoorthy, M. H. Lim, *J. Am. Chem. Soc.* **2009**, *131*, 16663.

[7] a) F. Bard, C. Cannon, R. Barbour, R. Burke, D. Games, H. Grajeda, T. Guido, K. Hu, J. Huang, K. Johnson-Wood, K. Khan, D. Kholodenko, M. Lee, I. Lieberburg, R. Motter, M. Nguyen, F. Soriano, N. Vasquez, K. Weiss, B. Welch, P. Seubert, D. Schenk, T. Yednock, *Nat. Med.* **2000**, *6*, 916; b) J. McLaurin, R. Cecal, M. E. Kierstead, X. Tian, A. L. Phinney, M. Manea, J. E. French, M. H. L. Lambermon, A. A. Darabie, M. E. Brown, C. Janus, M. A. Chishti, P. Horne, D. Westaway, P. E. Fraser, H. T. J. Mount, M. Przybylski, P. St George-Hyslop, *Nat. Med.* **2002**, *8*, 1263.

[8] a) C. Cabaleiro-Lago, F. Quinlan-Pluck, I. Lynch, S. Lindman, A. M. Minogue, E. Thulin, D. M. Walsh, K. A. Dawson, S. Linse, *J. Am. Chem. Soc.* **2008**, *130*, 15437; b) S. I. Yoo, M. Yang, J. R. Brender, V. Subramanian, K. Sun, N. E. Joo, S. Jeong, A. Ramamoorthy, N. A. Kotov, *Angew. Chem.* **2011**, *123*, 5216; *Angew. Chem. Int. Ed.* **2011**, *50*, 5110; c) J. Geng, M. Li, J. Ren, E. Wang, X. Qu, *Angew. Chem.* **2011**, *123*, 4270; *Angew. Chem. Int. Ed.* **2011**, *50*, 4184; d) B. Le Droumaguet, J. Nicolas, D. Brambilla, S. Mura, A. Maksimenko, L. De Kimpe, E. Salvati, C. Zona, C. Airoldi, M. Canovi, M. Gobbi, N. Magali, B. La Ferla, F. Nicotra, W. Scheper, O. Flores, M. Masserini, K. Andrieux, P. Couvreur, *ACS Nano* **2012**, *6*, 5866.

[9] a) J. Hardy, D. J. Selkoe, *Science* **2002**, *297*, 353; b) K. G. Mawuenyega, W. Sigurdson, V. Ovod, L. Munsell, T. Kasten, J. C. Morris, K. E. Yarasheski, R. J. Bateman, *Science* **2010**, *330*, 1774; c) K. P. Kepp, *Chem. Rev.* **2012**, *112*, 5193.

[10] a) I. Benilova, E. Karran, B. De Strooper, *Nat. Neurosci.* **2012**, *15*, 349; b) K. Ono, M. M. Condron, D. B. Teplow, *Proc. Natl. Acad. Sci. USA* **2009**, *106*, 14745.

[11] a) F. U. Hartl, A. Bracher, M. Hayer-Hartl, *Nature* **2011**, *475*, 324; b) F. U. Hartl, M. Hayer-Hartl, *Science* **2002**, *295*, 1852.

[12] a) S. L. Helfand, *Science* **2002**, *295*, 809; b) P. J. Muchowski, *Neuron* **2002**, *35*, 9; c) R. B. DeMattos, J. R. Cirrito, M. Parsadanian, P. C. May, M. A. O'Dell, J. W. Taylor, J. A. K. Harmony, B. J. Aronow, K. R. Bales, S. M. Paul, D. M. Holtzman, *Neuron* **2004**, *41*, 193.

[13] X. Liu, Y. Liu, Z. Zhang, F. Huang, Q. Tao, R. Ma, Y. An, L. Shi, *Chem. Eur. J.* **2013**, *19*, 7437.

[14] H. Gao, J. Xiong, T. Cheng, J. Liu, L. Chu, J. Liu, R. Ma, L. Shi, *Biomacromolecules* **2013**, *14*, 460.

[15] S. M. Butterfield, H. A. Lashuel, *Angew. Chem.* **2010**, *122*, 5760; *Angew. Chem. Int. Ed.* **2010**, *49*, 5628.

[16] a) Y. Fezoui, D. B. Teplow, *J. Biol. Chem.* **2002**, *277*, 36948; b) K. J. Marcinowski, H. Shao, E. L. Clancy, M. G. Zagorski, *J. Am. Chem. Soc.* **1998**, *120*, 11082.

[17] a) G. T. Dolphin, P. Dumy, J. Garcia, *Angew. Chem.* **2006**, *118*, 2765; *Angew. Chem. Int. Ed.* **2006**, *45*, 2699; b) P. Manavalan, W. C. Johnson, *Nature* **1983**, *305*, 831.

[18] a) Y. Kusumoto, A. Lomakin, D. B. Teplow, G. B. Benedek, *Proc. Natl. Acad. Sci. USA* **1998**, *95*, 12277; b) H. Li, B. H. Monien, A. Lomakin, R. Zemel, E. A. Fradinger, M. Tan, S. M. Spring, B. Urbanc, C. Xie, G. B. Benedek, G. Bitan, *Biochemistry* **2010**, *49*, 6358.

[19] M. R. Nilsson, *Methods* **2004**, *34*, 151.

[20] a) A. K. Buell, E. K. Esbjoerner, P. J. Riss, D. A. White, F. I. Aigbirhio, G. Toth, M. E. Welland, C. M. Dobson, T. P. J. Knowles, *Phys. Chem. Chem. Phys.* **2011**, *13*, 20044; b) M. K. Mustafa, A. Nabok, D. Parkinson, I. E. Tothill, F. Salam, A. Tsargorodskaya, *Biosens. Bioelectron.* **2010**, *26*, 1332.

[21] D. Brambilla, R. Verpillot, B. Le Droumaguet, J. Nicolas, M. Taverna, J. Kóňa, B. Lettiero, S. H. Hashemi, L. De Kimpe, M. Canovi, M. Gobbi, V. Nicolas, W. Scheper, S. M. Moghimi, I. Tvaroška, P. Couvreur, K. Andrieux, *ACS Nano* **2012**, *6*, 5897.

[22] a) T. Saido, M. A. Leissring, *Cold Spring Harbor Perspect. Med.* **2012**, *2*, a006379; b) Y. Wang, H. Zhou, X. Zhou, *Drug Discovery Today* **2006**, *11*, 931.

